Biochimica et Biophysica Acta, 1100 (1992) 242–250

BBABIO 43614

Laser-induced optoacoustic calorimetry of cyanobacteria. The efficiency of primary photosynthetic processes in state 1 and state 2

Doug Bruce and Omid Salehian

Department of Biological Sciences, Brock University, St. Catharines (Canada)

(Received 21 October 1991)
(Revised manuscript received 19 February 1992)

Key words: Photosynthesis; Optoacoustic; Photoacoustic; State transition; Energy storage; (Cyanobacterium)

The heat released by all primary processes of photosynthesis within 2 μs of a laser flash was measured by optoacoustic spectroscopy of the cyanobacteria *Synechococcus sp.* PCC 6301 adapted to state 1 and state 2. Heat production was compared between intact cells with open and closed reaction centres allowing direct determination of the efficiency of photosynthetic energy storage. The fraction of absorbed energy released as heat was the same for cells in state 1 and state 2 for excitation of either phycocyanin or chlorophyll *a*. We conclude that the efficiency of excitation energy transfer and primary photochemical energy storage was not affected by the state transition. These results contradict proposed models for the state transition in cyanobacteria, which involve the uncoupling of phycobilin pigments from energy transfer to chlorophyll *a*.

Introduction

State transitions

In oxygenic photosynthesis the distribution of excitation energy between Photosystem II (PS II) and Photosystem I (PS I) is regulated by the light state transition [1,2]. The state transition serves to control the activities of PS II and PS I by changing their effective absorbance cross-sections. Preferential excitation of PS II triggers the state transition mechanism to alter the distribution of excitation energy in favour of PS I (state 2). Preferential excitation of PS I changes the distribution to favour PS II (state 1). In this way the state transition has been proposed to balance the activities of PS II and PS I to optimize linear electron transport. The state transition can also be triggered by shifts in cell metabolism [3,4]. Metabolic demands for increased ATP/NADPH ratios have been correlated with increased excitation energy transfer to PS I, presumably increasing ATP production via PS I cyclic electron transport [4].

The mechanism of the state transition in chlorophyll *a*/*b* (Chl *a*/*b*)-containing organisms is based on differential association of the Chl *a*/*b* light-harvesting complex 2 (LHC2) between PS II and PS I. The proposed mechanism involves reversible phosphorylation of a fraction of LHC2. Transition to state 2 is associated with this phosphorylation. An LHC2 kinase is activated by preferential excitation of PS II via the reduction of plastoquinone (PQ) and/or the cytochrome b_6/f complex. The phosphorylation of LHC2 increases its affinity for PS I and decreases its affinity for PS II. A lateral migration of the phospho-LHC2 complex away from PS II-rich grana membrane regions towards PS I-rich stroma membrane regions ensues. This decrease in PS II absorbance cross-section and increase in PS I absorbance cross-section is characteristic of state 2. The transition to state 1 is the reverse process driven by a background phosphatase activity, see Ref. 1 for review.

Three mechanisms have been postulated for the state transition in phycobilisome (PBS)-containing organisms. The mechanisms agree on the organization of the photosynthetic apparatus in state 1. The PBS is preferentially associated with PS II and the rate of excitation energy transfer from PS II Chl *a* to PS I Chl *a* (spillover) is low or nonexistent. The mechanisms

Correspondence to: D. Bruce, Department of Biological Sciences, Brock University, St. Catharines, Ontario, Canada L2S 3A1.

Abbreviations: Chl, chlorophyll; PQ, plastoquinone; LHC, light-harvesting complex ; DCMU, 3-(3,4-dichlorophenyl)-1,1'-dimethylurea; LIOAS, laser-induced optoacoustic spectroscopy; PS, photosystem; P680, primary donor of Photosystem II; P700, primary donor of Photosystem I.

differ in the proposed changes in organisation of the photosystems and PBS on transition to state 2.

The mobile PBS model [5] is analogous to the mechanism described above for Chl *a/b* LHC2-containing organisms. Transition to state 2 is proposed to be driven by phosphorylation of the PBS which causes its dissociation from PS II and subsequent association with PS I. This increases the contribution of the PBS to the PS I absorbance cross-section at the direct expense of PS II. The distribution of energy absorbed by Chl *a* remains unchanged. This model is not supported by experiments which show that the distribution of energy absorbed by Chl *a* is affected by the state transition [1,2,6] and by the demonstration of a state transition in a PBS-less cyanobacterial mutant [7].

The spillover model [6,8,9] proposes that a change in the proximity of PS II and PS I controls the distribution of excitation energy between PS II Chl *a* and PS I Chl *a*. The response to preferential excitation of PS II is to move the photosystems closer together, increasing the probability of excitation energy transfer from the PS II Chl *a* antenna to PS I Chl *a* antenna (spillover). This results in an increase in the effective absorbance cross-section of PS I by contributions from both the PBS and PS II Chl *a*. Most support for this model comes from steady-state and time-resolved 77-K fluorescence spectroscopy [6,10,11].

The PBS detachment model [12] is a combination of the above models. Transition to state 2 is effected by phosphorylation of the PBS and PS II. The PBS leaves PS II and the two photosystems move closer together, increasing 'spillover'. The PBS remains detached from either photosystem and thus PBS contributions to the absorbance cross-sections of both photosystems are predicted to decrease. In contrast, the contribution of Chl *a* to the effective absorbance cross-section of PS I would increase via spillover from PS II Chl *a*. Evidence for the detachment of the PBS comes from room temperature Chl *a* fluorescence induction [12,13] and picosecond time-resolved fluorescence decay data [14]. In the PBS detachment model energy absorbed by the uncoupled PBS in state 2 is proposed to be 'quenched' and released as heat as no increase in PBS fluorescence has been observed [13,14]. The PBS detachment model proposes that the state transition is a photoprotective mechanism as far as PBS absorption is concerned.

The introduction of the PBS detachment model followed from fluorescence emission studies in which excitation absorbed by the PBS appeared to undergo larger changes in distribution than excitation absorbed by Chl *a* [12,13]. These results were not predicted by the spillover model. On the other hand, reports of increased contributions of the PBS to PS I in state 2 [6,15–17] are not consistent with PBS detachment. A recent quantitative study of 77 K fluorescence emission and excitation spectra of cyanobacteria has shown that the increased contribution of both PBS and Chl *a* to PS I in state 2 is much smaller than the decrease in their contributions to PS II [15]. It is clear that fluorescence measurements must be complemented by more direct measures to confirm the state transition-induced changes in the organization of the photosynthetic apparatus.

The PBS detachment model has raised a primary question about the nature of the state transition mechanism. Does the state transition act as a photoprotective mechanism by uncoupling antenna pigments from reaction centres? The most direct way to answer this question is to measure the amount of heat released in state 1 and state 2 for light absorbed by the PBS.

Pulsed laser-induced optoacoustic spectroscopy

Direct measurements of heat release and photosynthetic energy storage are possible with photoacoustic techniques. The most popular technique for measuring energy storage photoacoustically is the gas-coupled microphone [18]. A leaf or thin layer of algae is sealed into a gas-tight chamber and illuminated with a chopped light source. A modulated pressure signal is detected by the microphone and measured with the aid of a frequency selective amplifier. Both heat-induced volume expansion and oxygen evolution may contribute to the photoacoustic signal. However, they can be separated by analysis of the phase of the photoacoustic signal (the oxygen signal is slower) or by changing the frequency of the modulated light (the oxygen signal is attenuated at high frequency). On the millisecond time scale of this technique, heat release associated with all photosynthetic processes ranging from internal conversion in the antenna to secondary electron and proton transport processes associated with ATP production will contribute to the photoacoustic signal. Photoacoustic spectroscopy has been applied to state transition studies in intact cyanobacteria by following changes in PS II activity through detection of the photoacoustic oxygen signal [19]. State-transition-induced changes in photosynthetic energy storage in intact red algae on the millisecond time scale have also been determined with this technique [20].

In laser-induced optoacoustic spectroscopy (LIOAS) the heat released by a sample in solution after absorption of a short laser pulse is detected as an acoustic pulse by a piezoelectric crystal [21]. The time scale of the measurement is determined by the pulse width of the laser, time response of the piezoelectric crystal, and the travel time of the acoustic pulse in the solution over a distance equal to the diameter of the laser beam. The latter is usually limiting and is typically nanoseconds to microseconds [22]. In this time scale heat loss associated with the slower electron and proton transport processes does not contribute to the

optoacoustic signal. Thus, LIOAS is particularly well suited to determinations of the efficiencies of excitation energy transfer and primary processes in the reaction centres of PS II and PS I. Heat loss determinations from LIOAS can be calibrated by either an external standard, which emits all absorbed energy as heat, or in photosynthetic systems by comparing heat loss of open and closed reaction centres [22]. LIOAS is very convenient for use with algae as the energy storage determinations can be made with intact algal cells suspended in their growth medium [22].

In this report we have used LIOAS to measure the amount of energy stored by intact cells of cyanobacteria in state 1 and state 2 within 2 μs of excitation. We observe no difference in the amount of energy stored by the primary processes of photosynthesis in state 1 and state 2. Our results show no evidence for an uncoupling of the PBS from excitation energy transfer to the reaction centres and are thus in direct conflict with the PBS detachment model.

Materials and Methods

Sample preparation

Synechococcus sp. PCC 6301 was grown photoautotrophically at 30°C on BG-11 in batch culture and harvested in log phase, as described previously [23]. Cells were used at a Chl *a* concentration of 1–2 μg ml^{-1} and were suspended in growth media with 10% ethylene glycol. Ethylene glycol has a thermal expansion coefficient approx. 5-times higher than water and was added to improve signal-to-noise by increasing the amplitude of the optoacoustic signal [22]. The presence of 10% ethylene glycol in the suspension did not affect the integrity of the PBS or the cells' capacity to undergo state transitions as assayed by 77 K fluorescence spectroscopy.

State transitions in cyanobacteria can be driven by preferential excitation of PS II- and PS I-associated pigments or by direct manipulation of the redox state of PQ and/or cytochrome b_6/f. State 2 can be achieved in most cyanobacteria simply by dark adaptation, as respiratory electron transport activity keeps PQ and cytochrome b_6/f reduced in the dark [7]. State 1 is easily achieved by illumination of DCMU-treated cells to oxidize PQ and cytochrome b_6/f.

For each experiment a cell suspension (50 ml total) was circulated at a rate of 40 ml min^{-1} from a 40 ml waterjacketed glass reservoir to a 1 cm square glass cuvette (3 ml) and back with a peristaltic pump. Unless otherwise stated all experiments were done at 28°C. For state transition experiments 1 μM DCMU was added to the suspension. State 2 was achieved by keeping the cells in the dark and state 1 by illuminating the reservoir with white light (200 W m^{-2}). There was a 4 s dark interval between the reservoir and the measuring cuvette to allow reaction centres which had been closed by this illumination to open before measurement. When required, reaction centres were closed by direct illumination of the cuvette during measurement with 2000 W m^{-2} of white light. State transitions were verified by 77 K fluorescence spectroscopy. Samples (75 μl) were taken from the cuvette during the optoacoustic measurement just prior to the laser flash and quickly frozen in liquid nitrogen. 77 K fluorescence emission spectra were determined with the apparatus described previously [7].

LIOAS apparatus

The optoacoustic detector was built by the Brock University machine shop following the design of Tam and Patel [21]. Signal-to-noise was increased by using two lead zirconate titanate (PZT) piezoelectric crystals (Vernitron, Bedford, OH), one on either side of a 1-cm glass cuvette equidistant from the laser beam, as described by Nitsch et al. [22]. The two crystals were mounted with opposite polarity and their outputs added by a differential amplifier stage. A second amplifier stage similar to the one described by Braslavsky and Hiehoff [24], carried the signal to an Hitachi VC 6065 digital storage oscilloscope. The amplifiers were designed and constructed by the Brock University electronics shop.

Excitation flashes (250 ns duration) were generated by a Phase-R (New Durham, NH) DL-32 flash lamp pumped dye laser. The laser dye was either Rhodamine G (Phase-R), used at 590 nm or DCM (Exciton), used between 605 nm and 690 nm. The laser beam diameter was defined by a 3 mm diameter aperture which resulted in an effective acoustic transit time of 2 μs. The intensity of the exciting laser flash was attenuated with neutral density filters and a neutral density filter wedge. A beam splitter directed 50% of the laser flash to a laser pulse pyrometer (Molectron, Portland, OR) so the energy of each laser pulse (E) could be determined directly. Signals were averaged at lower flash energies up to 128 times. The flash frequency was 0.2 Hz.

Calculations of energy storage

Heat emission measured by LIOAS must be calibrated by external and/or internal standards. $CuCl_2$ can be used as a calorimetric standard as it releases all absorbed energy by heat emission within a few nanoseconds [22]. For $CuCl_2$ the fraction of absorbed energy released as heat, α, is equal to one and a $CuCl_2$ solution adjusted to the same absorbance as the sample acts as an external calibration or reference for maximal heat emission. Photosynthetically active samples can also be calibrated internally by determinations of heat emission when all reaction centres are closed. Under these conditions all energy absorbed by the antenna

pigments must be released as either heat or fluorescence. If the fluorescence yield is significant the fraction of absorbed energy emitted as heat, α, must be corrected for the fluorescence loss of the closed reaction centres as described below in Eqn. 1 [22].

$$\alpha = \{1 - \phi_f^{cl}\lambda_e/\lambda_f\}H_{op}/H_{cl} \quad (1)$$

where ϕ_f^{cl} is the fluorescence yield of closed reaction centres, λ_f and λ_e are the wavelengths of the weighted average of fluorescence and excitation, respectively, and H_{op} and H_{cl} are the energy normalized optoacoustic signal amplitudes of samples with open and closed reaction centres, respectively.

To a first approximation the amount of energy stored photosynthetically (ΔE) is simply $1 - \alpha$ if we assume a quantum yield of 1 for both reaction centres and that losses due to entropic changes and fluorescence from open reaction centres are insignificant. This energy storage can be easily corrected for internal conversion losses from the antenna pigment absorbing the excitation flash to the reaction centre by the factor λ_{trap}/λ_e where λ_{trap} is the wavelength of maximal absorption of the reaction centre photopigment and λ_e is the wavelength of the excitation flash. This will give the amount of energy storage as a fraction of the energy of P680/P680* or P700/P700* (ΔE_{rel}). To be exact a correction for the energy lost as fluorescence from open reaction centres, $\phi_f^{op}\ \lambda_e/\lambda_f$, should also be included. The relative energy storage is thus given by Eqn. 2 shown below:

$$\Delta E_{rel} = \lambda_{trap}/\lambda_e\{1 - \alpha\} - \phi_f^{op}\lambda_e/\lambda_f \quad (2)$$

As PS II and PS I are both contributing to energy storage in intact cells we chose 690 nm as an approximate value for λ_{trap}.

Results and Discussion

Fig. 1 shows an example of the optoacoustic signal generated by intact cells of cyanobacteria after absorption of a laser pulse. The amplitude of the first peak is proportional to the amount of heat released by the cells. The first peak is followed by a series of oscillations at the resonance frequency of the piezoelectric crystal. To improve the signal-to-noise we measured the distance from the top of the first peak to the bottom of the first trough (H) as the amplitude of the photoacoustic signal. Our results were independent of whether we measured the amplitude of the first peak or the distance H.

LIOAS of photosynthetic systems is potentially sensitive to acoustic pulses generated by both heat release and conformational changes induced by charge separation in the reaction centres. These two contributions

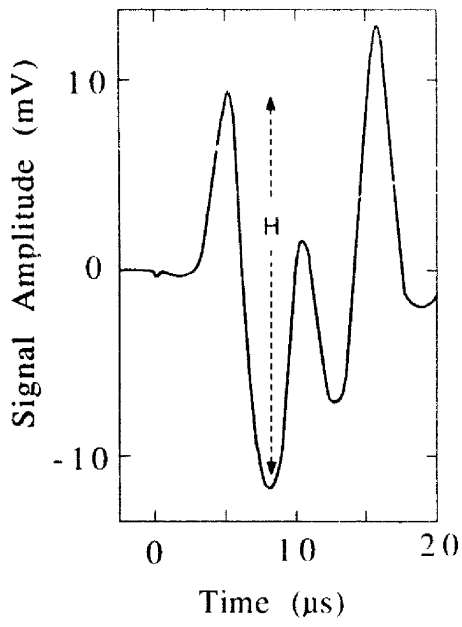

Fig. 1. Optoacoustic transient generated by intact cyanobacteria after absorption of a single 150-μJ laser flash. The laser was fired at time 0 μs on the trace. The distance H was taken as the amplitude of the acoustic pulse.

can theoretically be separated by measuring the acoustic signal at 4°C where water reaches maximum density and its thermal expansion coefficient is zero. In Fig. 2 we show for a $CuCl_2$ solution in distilled water, as

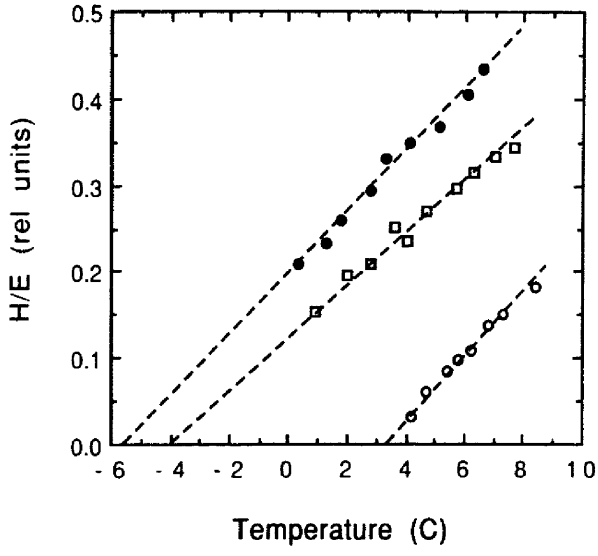

Fig. 2. Pulse energy normalized amplitude (H/E) of the acoustic pulse as a function of temperature for a 0.6 mM solution of $CuCl_2$ in distilled water, ○; the same solution of $CuCl_2$ with NaCl added to a final concentration of 0.5 M, ●; and a suspension of cyanobacteria in distilled water, □. The absorbance of the $CuCl_2$ solution was 0.22 at the excitation wavelength of 665 nm. The reaction centres of the cyanobacteria were closed by illumination of the cuvette during measurement as described in Materials and Methods. H/E was normalized to a value of one for intact cyanobacteria at 28°C.

previously described for water by Tam and Patel [21], that the acoustic signal decreased with temperature, effectively vanishing near 4°C (about 3°C in our experiment). The signal reappeared with the initial peak going negative instead of positive at temperatures below 3°C (data not shown). A change in the shape of the acoustic signal was expected as the thermal expansion coefficient for water is negative at temperatures below the maximum density temperature. In contrast, the acoustic signal generated by intact cyanobacteria suspended in distilled water decreased linearly with temperature but did not vanish near 4°C. Approximately 25% of the signal observed at 28°C was still present at 4°C. The initial peak of the acoustic pulse from the cyanobacteria continued to decrease below 4°C but remained positive down to the lowest temperature attainable. Extrapolation of the linear fit to the data indicates that zero signal would have occurred at approx. −4°C. The temperature dependence of the $CuCl_2$ optoacoustic signal could be made to mimic the cyanobacteria by the addition of NaCl. The temperature of the $CuCl_2$ solution where the optoacoustic pulse amplitude reached zero was depressed to approx. −5.5°C by the addition of 0.5 M NaCl. The temperature of maximum density was decreased by solutes in a manner analogous to the freezing point depression. The persistence of an acoustic signal below 4°C in the cyanobacteria may thus be explained by the high concentration of dissolved solutes in the interior of the cyanobacterial cell. The thermal expansion coefficient of the cell matrix will not be zero at 4°C and thermal expansion of the matrix may be acoustically coupled to the water suspending the cells through the cell wall. Although some contribution of conformational changes to the acoustic signal in intact cells is possible, the continuing linear decrease in amplitude of the acoustic signal below 4°C suggests that most of the acoustic signal is thermal.

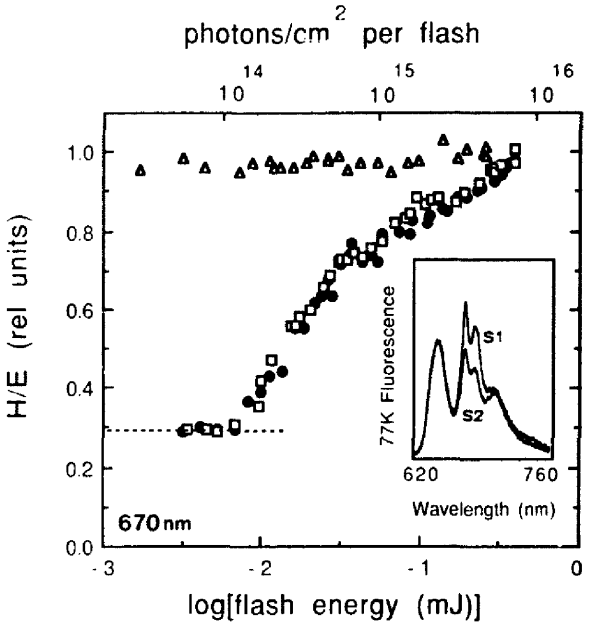

Fig. 4. Pulse energy normalized amplitude (H/E) of the acoustic pulse vs. log of the laser-flash energy (E) for intact cells of cyanobacteria. Cells with open reaction centres in state 1 (□) and state 2 (●) are compared to cells in state 1 with closed reaction centres (△), see Materials and Methods for details. The wavelength of the excitation flashes was 670 nm, chosen to excite Chl *a*. (- - - - -) shows the minimal value of H/E from open reaction centres, H_{op}. The inset shows 77 K fluorescence emission spectra (excitation wavelength, 590 nm) of samples of these cells in state 1 (S1) and state 2 (S2) removed during the optoacoustic measurement.

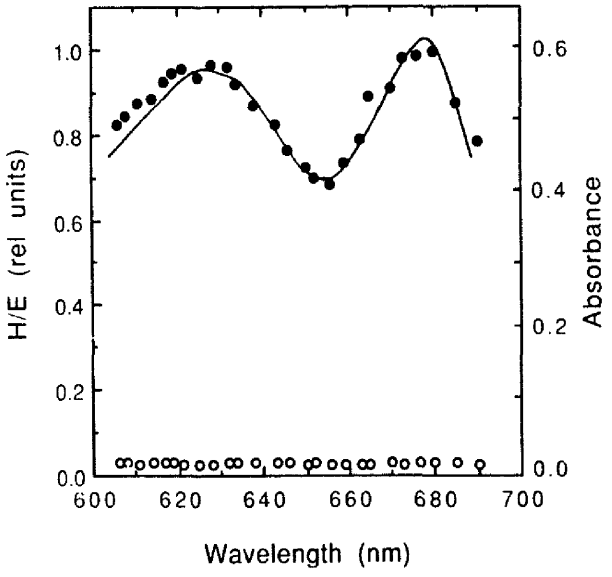

Fig. 3. Action spectra for the pulse energy normalized amplitude H/E of the acoustic signal in intact cyanobacteria with closed reaction centres, (●) and in cyanobacteria bleached by a 5 min exposure to a 10% solution of household bleach (○). Reaction centres were closed, as described in Materials and Methods. The scattering corrected absorbance spectrum of the same cells is shown by (———).

Action spectra for the pulse energy normalized amplitude (H/E) of the acoustic signal in intact cyanobacteria and bleached cyanobacteria are compared to the absorbance spectrum of intact cells in Fig. 3. The optoacoustic spectrum of intact cells closely matches the absorbance spectrum, with a phycocyanin peak at 625 nm and a Chl *a* peak at 675 nm. The small acoustic signal generated by scattering from the bleached cyanobacteria has a different waveform from that of intact cells or $CuCl_2$ (not shown) and is of much smaller amplitude.

The pulse energy normalized amplitude (H/E) of the acoustic signal for intact cyanobacteria with open reaction centres in state 1 and state 2 is compared to

that for cells with closed reaction centres in Fig. 4. The excitation wavelength was 670 nm, chosen to excite Chl *a*. Cells with closed reaction centres had a constant normalized heat loss over three orders of magnitude of flash energy that was independent of whether the cells were in state 1 or state 2 (not shown). This maximum value of H/E from closed reaction centres serves as an internal control and is referred to as H_{cl}. Cells with open reaction centres show much lower heat loss at low flash energies indicative of maximal photochemical energy storage. This minimum value of H/E is referred to as H_{op} and is shown by a dashed line on the figure. The relative amount of heat released increases with the flash energy as multiple hits begin to close a significant fraction of the reaction centres during the measurement. This continues until all reaction centres are closed early in the laser pulse and saturation is reached at H_{cl}. The complex sigmoidal shape of the open reaction centre curve reflects the absorbance cross-sections of both PS II and PS I.

We did not calculate absorbance cross-sections for heat loss from these curves. Absorbance cross-section calculations are frustrated by variations in laser flash intensity over the sample being measured. The optical arrangment required for the LIOAS setup is not optimal for these determinations. The long path length (1 cm) combined with the relatively high sample absorbance required for reasonable signal-to-noise (typically 0.6), resulted in a substantial decrease in laser flash intensity as the beam travels through the cuvette. In addition, the intensity of the laser beam was not homogeneous over its 3 mm diameter. Absorbance cross-sections estimated from our figures will be underestimates as the pulse intensities reported were those incident on the front surface of the cuvette.

There was no difference in the amplitude of the energy normalized optoacoustic pulse at low flash energies, H_{op}, or high flash energies, H_{cl}, or in the shape of the saturation curves for cells in state 2 and state 1. 77 K fluorescence emission spectra of cell samples taken during the measurement are shown in the inset and confirm that the cells were in state 1 and state 2.

In Fig. 5 the excitation wavelength was changed to 620 nm, to excite the PBS, and the experiment repeated with the same cells shown in Fig. 4. There was no difference in H_{op}, H_{cl} or in the shape of the saturation curves for cells in state 2 and state 1.

Fig. 6 shows an independent experiment on a different sample of cells where excitation of the PBS was accomplished at 590 nm, farther away from possible Chl *a* absorption on the short wavelength side of the PBS absorption. Again there was no difference in H_{op}, H_{cl} or in the shape of the saturation curves for cells in state 2 and state 1. State transitions were again confirmed by 77 K fluorescence emission spectra of cell samples taken during the measurement.

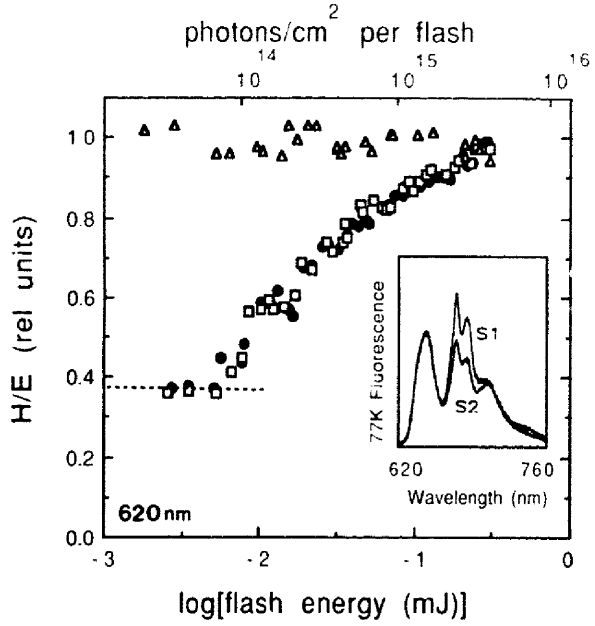

Fig. 5. Pulse energy normalized amplitude (H/E) of the acoustic pulse as a function of laser-flash energy (E) for intact cells of cyanobacteria. Cells with open reaction centres in state 1 (□) and state 2 (●) are compared to cells in state 1 with closed reaction centres (△), see Materials and Methods for details. The wavelength of the excitation flashes was 620 nm, chosen to excite the PBS. This experiment was done with the same cells used in Fig. 4. (- - - - - -) shows the minimum value of H/E from open reaction centres, H_{op}. The inset shows 77 K fluorescence emission spectra (excitation wavelength, 590 nm) of samples of these cells in state 1 (S1) and state 2 (S2) removed during the optoacoustic measurement.

Energy storage determinations

Figs. 4, 5 and 6 clearly show that the amplitudes of the acoustic pulses are essentially identical for cells in state 1 and state 2 for all flash intensities and for excitation of either Chl *a* or the PBS. As a first approximation these data indicate that the amount of energy storage is identical in state 1 and state 2.

Although the fluorescence yield of intact cells is small compared to the heat loss, a critical comparison of the fraction of absorbed energy lost as heat, α, in state 1 and state 2 requires consideration of the fraction of energy lost by fluorescence from cells with closed reaction centres ($\phi_f^{cl}\ \lambda_e/\lambda_f$) and open reaction centres ($\phi_f^{op}\ \lambda_e/\lambda_f$) in each state, as described in Methods by Eqn. 1 and Eqn. 2, respectively. Most of the Chl *a* fluorescence in intact photosynthetic systems originates from pigments associated with PS II and the maximum yield with closed reaction centres, ϕ_f^{cl}, calculated from fluorescence lifetime data from green algae is approx. 0.025 [25]. Fluorescence yields can be estimated by calculating the ratio of the fluorescence lifetime of Chl *a* in the intact cells to its natural fluorescence lifetime [25]. The fluorescence decay kinetics of intact cyanobacteria with open and closed

reaction centres in state 1 and state 2 have been measured by Mullineaux et al. [14]. They modelled the decay kinetics with a sum of exponential decays, $\Sigma A_i \tau_i$. Where A_i is the amplitude of the ith decay component and τ_i is the lifetime of ith decay component. We used the data of Mullineaux et al [14] to calculate the fluorescence yields of intact cells with open and closed reaction centres in state 1 and state 2 for excitation at 620 nm and 670 nm. We used the following equation adapted from Beddard et al. [25]:

$$\phi_f = \Sigma A_i \tau_i / \tau_0 \qquad (3)$$

Where ϕ_f is the fluorescence yield and τ_0 is the native lifetime (19.5 ns) of Chl *a* [25]. The amplitudes, A_i, were normalized so that $\Sigma A_i = 1$.

The fluorescence yields for excitation in the Chl *a* absorption region (670 nm) were, $\phi_f^{cl} = 0.008$ and $\phi_f^{op} = 0.004$ for cells in state 2 and $\phi_f^{cl} = 0.012$ and $\phi_f^{op} = 0.006$ for cells in state 1. The fluorescence yields for excitation of the PBS were, $\phi_f^{cl} = 0.014$ and $\phi_f^{op} = 0.012$ for cells in state 2 and $\phi_f^{cl} = 0.025$ and $\phi_f^{op} = 0.014$ for cells in state 1. The Chl *a* fluorescence yield is relatively smaller in cyanobacteria than green algae [25], as most of the Chl *a* is associated with PS I which has a much lower fluorescence yield than PS II.

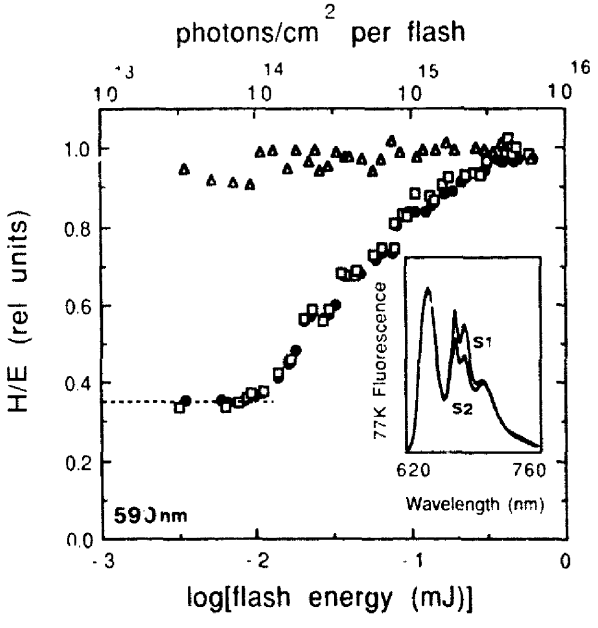

Fig. 6. Pulse energy normalized amplitude (H/E) of the acoustic pulse as a function of laser-flash energy (E) for intact cells of cyanobacteria. Cells with open reaction centres in state 1 (□) and state 2 (●) are compared to cells in state 1 with closed reaction centres (△), see Materials and Methods for details. The wavelength of the excitation flashes was 590 nm, chosen to excite the PBS. This was an independent repetition of the experiment in Figs. 4 and 5. (- - - - -) shows the minimum value of H/E from open reaction centres, H_{op}. The inset shows 77 K fluorescence emission spectra (excitation wavelength, 590 nm) of samples of these cells in state 1 (S1) and state 2 (S2) removed during the optoacoustic measurement.

TABLE I

Comparison of the ratio of acoustic pulse amplitudes for open and closed reaction centres (H_{op}/H_{cl}), the fraction of absorbed energy released as heat (α), and the relative amount of energy storage by PS II and PS I (ΔE_{rel}), for intact cells in state 1 and state 2 for excitation at 590 nm, 620 nm and 670 nm

α and ΔE_{rel} were calculated from H_{op}/H_{cl} using Eqn. 1 and Eqn. 2 in Materials and Methods. Values of H_{op}/H_{cl} are the averages of at least three independent experiments, standard errors are shown. The values used for ϕ_f^{cl}, ϕ_f^{op}, λ_e/λ_f and λ_{trap}/λ_e are given in the text.

	H_{op}/H_{cl}	α	ΔE_{rel}
590 nm			
State 2	0.47 ± 0.09	0.46 ± 0.09	0.62 ± 0.09
State 1	0.47 ± 0.09	0.46 ± 0.09	0.62 ± 0.09
620 nm			
State 2	0.43 ± 0.04	0.42 ± 0.04	0.63 ± 0.04
State 1	0.43 ± 0.04	0.42 ± 0.04	0.63 ± 0.04
670 nm			
State 2	0.28 ± 0.05	0.28 ± 0.05	0.74 ± 0.05
State 1	0.28 ± 0.05	0.28 ± 0.05	0.74 ± 0.05

For PBS excitation the weighted fluorescence emission peak was at 670 nm, therefore $\lambda_e/\lambda_f = 0.93$ for excitation at 620 nm and 0.88 for excitation at 590 nm. For Chl *a* excitation at 670 nm the weighted fluorescence emission peak was at 685 nm, so $\lambda_e/\lambda_f = 0.98$.

Table I shows H_{op}/H_{cl}, the fraction of absorbed energy released as heat, α, and the relative energy storage, ΔE_{rel}, for cells in state 1 and state 2. Values of H_{op}/H_{cl} in Table I are the averages of at least three independent experiments for each excitation wavelength. There was considerable variation in the value of H_{op}/H_{cl} between experiments performed on different samples on different days. The standard errors in Table I express this sample to sample variation. Variations in H_{op}/H_{cl} between states in any individual experiment (using one sample for both states) were much lower than the quoted standard error. Values for α and ΔE_{rel} were calculated from H_{op}/H_{cl} by equation 1 and equation 2, as described in Methods, using the above values for ϕ_f^{cl}, ϕ_f^{op} and λ_e/λ_f.

Our value of H_{op}/H_{cl} for excitation at 620 nm was the same for cells in state 1 or state 2 (0.43 ± 0.04) and was close to that reported by Nitsch et al. [22] for intact cells excited at 628 nm (0.4). Our determination of H_{op}/H_{cl} for excitation at 670 nm for cells in state 1 or state 2 (0.28 ± 0.05) was similar to their value for isolated PS I particles at 677 nm (0.25). However, our value was dramatically different from their value of 0.65 for intact cells excited with 677 nm flashes. We repeated our Chl *a* excitation experiment increasing

the wavelength of excitation from 670 nm to 677 nm and found a dramatic increase in H_{op}/H_{cl} to 0.58 ± 0.05 (not shown), much closer to the results of Nitsch et al. [22]. We would expect H_{op}/H_{cl} for excitation of Chl *a* in intact cells to be similar to the H_{op}/H_{cl} of PS I as most of the Chl *a* is associated with PS I in cyanobacteria. This is apparently not true for excitation of the long wavelength side of the Chl *a* Q_y absorption band. The unexpected increase in heat emission with increasing flash wavelength reflects a heterogeneity in the Chl *a* antenna which is currently under further investigation.

As expected, α was significantly larger for excitation of the phycobilisome at 590 nm (0.46) and 620 nm (0.42) than it was at 670 nm (0.28). Most of this was due to higher internal conversion losses and fluorescence losses in the PBS. However, values for ΔE_{rel}, which have been corrected for internal conversion and fluorescence losses, showed a larger energy storage for 670 nm excitation (0.74) than 590 (0.62) or 620 nm excitation (0.63). This is consistent with the relative distribution of PBS and Chl *a* absorbed excitation energy to PS II and PS I, respectively, as the energy storage capacity of PS I is higher than that of PS II on the 2 μs time scale of our experiment [22]. Our values of ΔE_{rel} for PBS excitation and Chl *a* excitation were slightly lower than, but comparable to, the values of relative energy storage reported for isolated PS II (0.65) and isolated PS I (0.83), respectively, by Nitsch et al. [22].

In none of our experiments was there a significant difference in H_{op}/H_{cl} between cells in state 1 and state 2, for excitation of either the PBS or Chl *a* Correction of H_{op}/H_{cl} for the different fluorescence losses in state 1 and state 2 did not result in significant differences in α or ΔE_{rel} between states. Our results show directly that the efficiency of excitation energy transfer and primary photochemistry within 2 μs of light absorption in cyanobacteria is the same in state 1 and state 2. Our data does not support the PBS detachment model which predicts a decrease in the efficiency of energy transfer from the PBS to Chl *a* and thus an increase in α in state 2 [13,14].

Measurements of heat release on a millisecond time scale with photoacoustic spectroscopy by Malkin et al. [20] have shown increased energy storage in state 2 in red algae. The time scale of their measurements was approx. 10 ms so additional heat loss associated with secondary electron transport and phosphorylation contributed to their energy storage determinations. If we assume similar mechanisms for the state transition in red algae and cyanobacteria the two experiments localize the changes in energy storage determined by Malkin et al. [20] to secondary electron transport and/or phosphorylation processes occurring in the time-range between 2 μs and 10 ms.

Addendum. What is the mechanism of the state transition?

Since the submission of this report a similar LIOAS study was published by Mullineaux et al. [26]. In agreement with this report they saw no difference in heat loss between intact cells in state 1 and state 2. Mullineaux et al. [26] also concluded that the PBS detachment model was incorrect, however they suggest that the PBS is still detached from PS II in state 2, based on fluorescence lifetime data from Mullineaux et al. [14]. They suggest that the detached PBS moves to PS I as described originally by the mobile PBS model. Another manuscript published since submission of our report, by Mullineaux and Holzwarth [27], describes a more detailed study of fluorescence lifetimes in cyanobacteria in state 1 and state 2. In this study excitation spectra for fluorescence decay kinetics attributed to PS II show a decrease in the contribution of PBS relative to Chl *a*. These data again support the idea of a decrease in the association of the PBS with PS II in state 2. However, the authors conclude that their analysis could not determine directly whether or not the PBS was attached to PS I in state 2.

Does the PBS detach from PS II and associate with PS I? As stated in the introduction to this report, the simple mobile PBS model is not supported by numerous experiments which have shown that the distribution of energy absorbed by Chl *a* is affected by the state transition [1,2,6] and by the demonstration of a state transition in a PBS-less cyanobacterial mutant [7]. Spillover from PS II to PS I must also be included to explain changes in the distribution of energy absorbed by Chl *a*.

Unfortunately, the spillover model, or a model combining both spillover and mobile antenna mechanisms, cannot explain all of the data. The fluorescence lifetime data of Mullineaux et al. [14, 27] are not consistent with a simple spillover mechanism. In addition, we have recently shown that the observed increase in contribution of the PBS to the 77 K fluorescence excitation spectrum of PS I in state 2 is much lower than what would be predicted by either the mobile PBS or spillover models for the state transition [15].

It is clear that none of the three proposed mechanisms for the state transition in cyanobacteria (mobile antenna, spillover and PBS detachment) can fully explain the data. Critical measurements of PS II and PS I activity are essential in determining functional changes in the distribution of excitation energy. We are currently working towards this goal.

Acknowledgments

We would like to thank Professor Silvia Braslavsky for sharing technical information about the components and construction of the piezoelectric transducer

and amplifier. We would also like to thank Meinhart Benkel, John Rustenberg, Roland Seehagal, and Gary McDonnell for their expert technical assistance in constructing components of the optoacoustic spectrometer. This work was supported by an equipment grant and operating grant from the Natural Sciences and Engineering Research Council of Canada to D.B. O.S. gratefully acknowledges the support of an Ontario Graduate Scholarship.

References

1 Williams, W.P. and Allen, J.F. (1987) Photosynth. Res. 13, 19–45.
2 Biggins J. and Bruce, D. (1989) Photosyn. Res. 20, 1–34.
3 Fernyhough, P., Foyer, C. and Horton, P. (1983) Biochim. Biophys. Acta 725, 155–161.
4 Turpin, D.H. and Bruce, D. (1990) FEBS Lett. 263, 99–103.
5 Allen, J.F. and Holmes, N.G. (1986) FEBS Lett. 202, 175–181.
6 Ley, A.C. and Butler, W.L. (1980) Biochim. Biophys. Acta 592, 349–363.
7 Bruce, D., Brimble, S. and Bryant, D.A. (1989) Biochim. Biophys. Acta 974, 66–73.
8 Murata, N. (1969) Biochim. Biophys. Acta 172, 242–251.
9 Biggins, J., Campbell, C.L. and Bruce, D. (1984) Biochim. Biophys. Acta 767, 138–144.
10 Bruce, D., Biggins, J., Steiner, T. and Thewalt, M. (1985) Biochim. Biophys. Acta 806, 237–246.
11 Bruce, D., Hanzlik, C., Hancock, L.A., Biggins, J. and Knox, R.S. (1986) Photosyn. Res. 10, 283–290.
12 Mullineaux, C.W. and Allen, J.F. (1988) Biochim. Biophys. Acta 934, 96–107.
13 Mullineaux, C.W. and Holzwarth, A.R. (1990) FEBS Lett. 260, 245–248.
14 Mullineaux, C.W., Bittersmann, E., Allen, J.F. and Holzwarth, A.R. (1990) Biochim. Biophys. Acta 1015, 231–242.
15 Salehian, O., and Bruce, D. (1992) J. Luminesc., 51, 91–98.
16 Fork, D.C., Murata, N. and Sato, N. (1979) Plant Physiol. 63, 524–530.
17 Tsinoremus, N.F., Hubbard, J.A.M., Evans, M.C.W. and Allen, J.F. (1989) FEBS Lett. 256, 106–110.
18 Malkin, S. and Cahen, D. (1979) Photochem. Photobiol. 29, 803–813.
19 Cannani, O. (1986) Biochim. Biophys. Acta 852, 74–80.
20 Malkin, S., Herbert, S.K. and Fork, D.C. (1990) Biochim. Biophys. Acta 1016, 177–189.
21 Tam, A.C. and Patel, C.K.N. (1979) Appl. Optics 18, 3348–3358.
22 Nitsch, C., Braslavsky, S.E. and Schatz, G.H. (1988) Biochim. Biophys. Acta 934, 201–212.
23 Brimble, S. and Bruce, D. (1989) Biochim. Biophys. Acta 973, 315–323.
24 Braslavsky, S.E. and Heihoff, K. (1989) in Handbook in Organic Photochemistry (Sciano, J., ed.), pp. 327–355, CRC, Boca Raton.
25 Beddard, G.S., Fleming, G.R., Porter, G., Searle, G.F.W. and Synowiec, J.A. (1979) Biochim. Biophys. Acta 545, 165–174.
26 Mullineaux, C.W., Griebenow, S. and Braslavsky, S. (1991) Biochim. Biophys. Acta 1060, 315–318.
27 Mullineaux, C.W. and A.R. Holzwarth (1991) Biochim. Biophys. Acta 1098, 68–78.